

## Mutant p53 R248Q but not R248W enhances *in vitro* invasiveness of human lung cancer NCI-H1299 cells

Kazuhito YOSHIKAWA<sup>1,2</sup>, Jun-ichi HAMADA<sup>2</sup>, Mitsuhiro TADA<sup>2</sup>, Takeshi KAMEYAMA<sup>2,3</sup>, Koji NAKAGAWA<sup>2,4</sup>, Yukiko SUZUKI<sup>2</sup>, Mayumi IKAWA<sup>2</sup>, Nur Mohammad Monsur HASSAN<sup>2</sup>, Yoshimasa KITAGAWA<sup>1</sup>, and Tetsuya MORIUCHI<sup>2</sup>

<sup>1</sup>Oral Diagnosis and Oral Medicine, Department of Oral Pathological Science, Graduate School of Dental Medicine, Hokkaido University, Kita-13, Nishi-7, Kita-ku, Sapporo 060-8586; <sup>2</sup>Division of Cancer-Related Genes, Institute for Genetic Medicine, Hokkaido University, Kita-15, Nishi-7, Kita-ku, Sapporo 060-0815; <sup>3</sup>Geriatric Stomatology, Department of Oral Pathological Science, Graduate School of Dental Medicine, Hokkaido University, Kita-13, Nishi-7, Kita-ku, Sapporo 060-8586; and <sup>4</sup>Department of Pathophysiology and Therapeutics, Graduate School of Pharmaceutical Science, Hokkaido University, Kita-12, Nishi-7, Kita-ku, Sapporo 060-0812, Japan

(Received 6 October 2010; and accepted 15 October 2010)

### ABSTRACT

More than half of all human cancers are associated with mutations of the *TP53* gene. In regard to the functional interaction with the remaining wild-type (WT) p53 allele, p53 mutations are classified into two types, recessive and dominant-negative (DN) mutations. The latter mutant protein has a DN activity over the remaining WT allele. We previously showed that the DN p53 mutant was useful as a predictor of poor outcome or a risk factor for metastatic recurrence in patients with some types of cancers, regardless of the presence or absence of loss of heterozygosity (LOH) of WT p53, suggesting that the DN p53 had ‘gain-of-function (GOF)’ activity besides the transdominance function. In this study, we investigated GOF activity of two DN p53 mutants which had a point mutation at codon 248 (R248Q and R248W), one of the hot spots, by transfecting them respectively into H1299 cells which originally expressed no p53 protein. Growth activity of the transfectants with the two mutants was not different from that of parent or Mock transfectants. Meanwhile, *in vitro* invasions of Matrigel and type I collagen gel by R248Q-transfectants were significantly higher than those by R248W-transfectants or the control cells. However, there were no differences in cell motile activities, expressions of extracellular matrix-degradative enzymes such as matrix metalloproteinases, urokinase-type plasminogen activator and heparanase, and their inhibitors, between R248Q- and R248W-transfectants. These findings indicate that the p53 mutants have a different quality in GOF activities even if the mutations occurred at the same codon. And detailed information of the status of p53, including transdominancy and GOF activity, is expected to be useful for diagnosis and therapeutic strategy fitting the individual patients.

*TP53* tumor suppressor gene encodes a transcription factor (p53), which forms homotetramer and binds to DNA in a sequence-specific manner to transcribe target genes. It is well known that genotoxic stress induces the stabilization and activation of the p53

protein, resulting in apoptosis, inhibition of cell-cycle progression, differentiation, senescence, or accelerated rates of DNA repair (18). More than half of all human cancers are associated with alterations of the *TP53* gene (7). Most *TP53* alterations are missense mutations, localized in the DNA-binding domain, and abolish the transcriptional activity via p53-responsive element. The residues such as R175, G245, R248, R249, R273 and R282 in the p53 protein are frequently mutated, which called “hot spots” (7). In their functional interactions with the remain-

Address correspondence to: Jun-ichi Hamada, Division of Cancer-Related Genes, Institute for Genetic Medicine, Hokkaido University, Kita-15, Nishi-7, Kita-ku, Sapporo 060-0815, Japan  
E-mail: jhamada@igm.hokudai.ac.jp

ing wild-type (WT) p53 allele, the p53 mutations are classified into two types, recessive (R) and dominant-negative (DN) mutations. DN p53 mutants inactivate the endogenous WT p53 protein in a DN fashion by forming heterotetramer complex (12, 13). We previously reported that the DN p53 mutant was available as a predictor of poor outcome in cancer patients. For example, in endometrial cancers of uterus, DN p53 mutation is a strong predictor of survival of patients since it is often found in advanced stages and aggressive histologic subtypes (21). DN p53 mutations are related to early onset of glioblastoma multiforme (10), and also a risk factor for metastatic recurrence in patients with oral squamous cell carcinomas (8). Such correlations between DN p53 mutations and poor prognosis are found even in the absence of the WT p53 allele due to loss of heterozygosity (LOH). These findings suggest that DN p53 mutations acquire new functions ("gain-of-function", GOF) related to malignancy other than transdominance over WT p53 function. Indeed, some DN p53 mutants are known to bind to other transcription factors and to transactivate or repress specific target genes, such as *MYC* (6), *MDR-1* (22), *CD95 (Fas/APO-1)* (26), *EGR1* (25), and so on. It is important to understand malignant properties acquired by GOF activity in each mutation so that we could make better use of genetic information for diagnosis and therapy.

R248 is localized in DNA-binding domain, and is well known as one of the targets of hot spot mutations. It is converted into three kinds of amino acid, R248Q, R248W and R248L, by point mutation in a variety of cancers (20). Although each of the mutants is known to inactivate the transactivational functions of WT p53, its GOF in tumor malignancy remains obscure. In this study, we enforced the expression of R248Q or R248W in p53-null human cancer cells (NCI-H1299) and compared the *in vitro* malignant behaviors, especially metastasis-related properties, between them.

## MATERIALS AND METHODS

**Cell lines and cell culture.** Human non-small cell lung cancer NCI-H1299 cells were purchased from American Type Culture Collection (ATCC, Chicago, IL). Human choriocarcinoma BeWo cells and human skin squamous cell carcinoma HSC-1 cells were obtained from Health Science Research Resource Bank (Sennan, Osaka, Japan). The cells were grown on Dulbecco's modified Eagle's minimum essential medium and Ham's F12 medium (D-MEM/Ham's

F-12) containing 10% fetal bovine serum (FBS). The cell lines were cultured in CO<sub>2</sub> incubator (5% CO<sub>2</sub> and 95% air).

**Plasmid construction.** Mutant *TP53*-expressing plasmids were made by inserting a fragment of the coding region of *TP53* with point mutation into the pIRES2-AcGFP1 plasmid vector (Clontech, Mountain View, CA). First, the insert (fragment of p53 codon 1 to 99) was amplified by PCR using pSS16-wild type *TP53* (10) template with addition of *NheI* and *XhoI* restriction sites to primers matching those found in the pIRES2-AcGFP1 vector. The following primers were used: forward, 5'-TATGCTAGCATG GAGGAGCCGCAGTC-3' and reverse, 5'-ATACT CGAGGAAGGGACAGAAGATGACAGG-3'. Restriction digest with *NheI* and *XhoI* enzymes was performed on both the insert and vector, followed by ligation with T4 DNA ligase (pIRES2-AcGFP1 p53 (1-99)). Next, the other insert (fragment of p53 codon 82 to 394) was excised from pSS16 R248Q (10) and pSS16 R248W (10) respectively by restriction digest with *SgrAI* and *SacI* enzymes. The insert was ligated into pIRES2-AcGFP1 p53 (1-99) which had been digested with *SgrAI* and *SacI* enzymes (pIRES2-AcGFP1 p53 R248Q and pIRES2-AcGFP1 p53 R248W). The control vector to pIRES2-AcGFP1 p53 R248Q and pIRES2-AcGFP1 p53 R248W was constructed as follows: The DNA fragment composed of sense DNA (5'-CCGGCGTGAG CGCCTCCATGAGAGCT-3') and antisense DNA (5'-CTCATGGAGGCGCTCACG-3') was inserted into pIRES2-AcGFP1 p53 (1-99) which had been digested with both *SgrAI* and *SacI* enzymes. This control vector was designed to express stop codon at 84th codon (pIRES2-AcGFP1 p53 (1-83)).

**Transfection and cell cloning.** H1299 cells were transfected with pIRES2-AcGFP1 p53 R248Q, pIRES2-AcGFP1 p53 R248W, or pIRES2-AcGFP1 p53 (1-83) by using Lipofectamine 2000 reagent (Invitrogen, Carlsbad, CA) according to manufacturer's instructions. The stably transfected cells were selected in the medium containing 250 µg/mL G418 sulfate (Cellgro, Herndon, VA). Cell cloning of the stable transfectants was performed by picking up a single grown colony with a small piece of filter paper containing trypsin/EDTA.

**Yeast p53 functional assay.** The yeast functional assay was performed according to our previous method (5, 24). Colorimetric evaluation of yeast colonies (red or white colonies) was done after 48 h culture.

To confirm mutations, we collected the pSS16 plasmids containing a mutant *TP53* from red yeast colonies, and then transfected the plasmids into XL-1 blue *E. coli* by electroporation. The plasmids were recovered, purified, and sequenced with BigDye<sup>®</sup> Terminator 3.1 Cycle Sequencing Kit (Applied Biosystems, Foster city, CA) on ABI PRISMS 3100-avant genetic analyzer (Applied Biosystems).

**Immunofluorescence.** Tumor cells ( $2.5 \times 10^4$ /well) were seeded on an 8-well chamber slide (Iwaki, Nagoya, Japan). After overnight incubation, the cells were fixed in 4% paraformaldehyde for 15 min at room temperature, permeabilized with 0.1% Triton X-100 for 5 min, and incubated for blocking with 3% BSA for 10 min. They were sequentially incubated with a mouse monoclonal antibody to p53 (DO-1; MBL, Nagoya, Japan) for 30 min at room temperature and with Alexa Fluor 568 goat anti-mouse IgG (Invitrogen) as a secondary antibody. After nuclear staining with DAPI (WAKO, Osaka, Japan), the cells were analyzed with a Fluoview FV5000 laser scanning confocal microscope (Olympus, Melville, NY).

**Cell proliferation assay.** Cell proliferation assay was performed by using a colorimetric crystal violet-staining procedure (9) with modification. Tumor cells were seeded on a 96-well plate in D-MEM/Ham's F-12 supplemented with 10% FBS. One and 3 days after the cell seeding, the medium was removed and all the wells were washed twice with 50  $\mu$ L/well PBS. The cells were then fixed with 50  $\mu$ L/well 5% glutaraldehyde for 30 min. The fixative was removed and the cells were stained with 50  $\mu$ L/well 50 mM 3-Cyclohexylamino-1-propane-sulfonic acid (CAPS) buffered solution containing 0.1% crystal violet for 30 min. The wells were then washed with MilliQ water, dried, and the stained cells were solubilized with 50  $\mu$ L/well 10% acetic acid for 15 min. For determining the cell number the absorbance of each well was measured at 590 nm on Microplate reader (Bio-Rad Laboratory, Hercules, CA). Each data was represented as the mean  $\pm$  SD of triplicate wells. Absorbance values obtained by crystal violet assay were linearly correlated with cell numbers within a range from 100 cells/well to 20,000 cells/well.

**In vitro invasion assay.** We carried out two types of *in vitro* invasion assays in this study (14). Matrigel invasion assay was performed by using a Matrigel invasion chamber (BD Biosciences, Bedford, MA).

Before the assay, Matrigel was rehydrated by adding D-MEM/Ham's F-12 into upper and lower compartments of the invasion chambers for 2 h. The medium in the upper compartment was replaced into 500  $\mu$ L of cell suspension ( $4 \times 10^4$ /mL, D-MEM/Ham's F-12 supplemented with 10% FBS). Into the lower compartment of the chamber, 750  $\mu$ L of D-MEM/Ham's F-12 supplemented with 10% FBS was placed. After 24 h- or 48 h-incubation, each membrane was fixed with 10% neutral-buffered formalin and stained in Giemsa solution. After the cells attached to the upper side of the membrane were removed by wiping with a cotton swab, those attached to the lower side of the membrane were counted under a microscope. Invasiveness of the cells was evaluated by the number of the cells penetrating the membrane. Each data was represented as the mean  $\pm$  SD of triplicate wells. Invasion of type I collagen gel by tumor cells was performed by using Transwell chambers with 8  $\mu$ m pore-membrane (Corning, Corning, NY). Type I collagen solution (Cellmatrix type I-A; Nitta Gelatin, Yao, Japan), 10-fold concentrated D-MEM, NaHCO<sub>3</sub>/HEPES and FBS were mixed in volume at 9 : 1 : 1 : 0.5, respectively. The mixed collagen solution (600  $\mu$ L) was placed in each well of 24-well plates, and a Transwell was placed onto each well. The Transwells were pressed down to make sure their tight contact with the collagen solution. After gelation in a CO<sub>2</sub> incubator, 100  $\mu$ L of cell suspension ( $2 \times 10^5$ /mL, D-MEM/F12 containing 10% FBS) was placed into the upper compartment of each Transwell. After 24 h-incubation in a CO<sub>2</sub> incubator, the Transwell was removed and the cells in the collagen gel were observed under an inverted phase-contrast microscope. Invasiveness was evaluated from the number of cells per field ( $\times 200$ ). Each data was represented as the mean  $\pm$  SD of total 10 fields.

**Chemotaxis assay.** Chemotaxis assay was performed by using Transwell chambers. In the lower compartment of the Transwell chambers, 600  $\mu$ L of D-MEM/Ham's F-12 containing (1) 1 mg/mL of BSA and 10  $\mu$ g/mL of bovine plasma fibronectin (Sigma, St. Louis, MO), (2) 1 mg/mL of BSA and 10  $\mu$ g/mL of bovine plasma vitronectin (Yagai, Yamagata, Japan), or (3) 1 mg/mL of BSA and 10  $\mu$ g/mL of mouse laminin-1 (Gibco BRL, Grand Island, NY) was placed, and then 100  $\mu$ L of cell suspension ( $2 \times 10^5$ /mL, D-MEM/Ham's F-12 containing 1 mg/mL of BSA) was placed into the upper compartment. After 6-h incubation, the assay was terminated, and cell migratory activity was evaluated in the same man-

ner as the invasion assay.

**In vitro wound-healing assay.** For measuring cell migrating activity, *in vitro* wound-healing assay was carried out according to the method described in our previous report (17) with some modification. Briefly, confluent cell monolayers were obtained after 36-h culture in D-MEM/Ham's F-12 supplemented with 10% FBS. They were gently scratched with a Gilson pipette yellow tip, and extensively rinsed with D-MEM to remove all cellular debris. This procedure left a cell-free area of substratum ('wound'). Then the cultures were observed with a phase-contrast inverted microscope and photographed.

**Western blot analysis.** Tumor cells were seeded at a density of  $5 \times 10^5$ /100-mm dish in D-MEM/Ham's F-12 supplemented with 10% FBS. After 24-h incubation, the cells were washed with 10 mL of cold PBS, and then harvested with a cell scraper in lysis buffer [50 mM Tris-HCl, pH 8.0, 150 mM NaCl, 1% NP40 containing 2% Complete mini (EDTA-free) Protease inhibitor cocktail Tablets] (Roche, Indianapolis, IN). The cell lysates were centrifuged at  $17,400 \times g$  for 15 min at 4°C. The supernatants were collected, and subjected to SDS-PAGE in 10% polyacrylamide gel and electrotransferred to Immobilon membranes (Millipore, Bedford, MA). The membranes were blocked in TBS-T (20 mM Tris-HCl, pH 7.5, 137 mM NaCl, 0.6% Tween 20) with 10% skim milk for 1 h at room temperature, and then incubated with primary antibodies (p53 DO-1; MBL) for 1 h at room temperature. The membrane was next incubated with horseradish peroxidase (HRP)-conjugated antibody to mouse IgG for 1 h at room temperature. Antigen-antibody complexes were visualized with Chemiluminescent HRP Substrate (Millipore).

**RNA preparation and quantitative real-time RT-PCR.** Total RNA was extracted from  $5 \times 10^5$  cells by using TRIzol reagent (Invitrogen). Reverse transcription was done for 1.5 µg total RNA, and the cDNA was synthesized by using Taqman Reverse Transcription Reagents (Applied Biosystems). Real-time PCR amplification was performed on 10 µL reaction mixture containing 1 µL cDNA sample, 5 µL QuantiFast SYBER Green Master Mix (QIAGEN, Valencia, CA) and with specific primer sets. PCR was carried out in a 7900 HT thermal cycler (Applied Biosystems, Warrington, UK) under the following conditions: 95°C for 5 min; then 40 cycles at 95°C for 10 s, and 61°C for 30 s. Dissociation curve anal-

ysis (95°C for 15 s, 60°C for 15 s 95°C 15 s) was performed at the end of the 40 cycles to verify the PCR product identity. Data were collected and analyzed with Sequence Detector Systems version 2.0 software (Applied Biosystems). The relative mRNA expression data were normalized to  $\beta$ -actin. The sequences of primers for *MMPs*, *TIMPs*, and *RECK* were as previously reported (1).

**Conventional RT-PCR.** Total RNA was extracted as described above. PCR amplification was performed in 20 µL reaction mixture containing 1 µL cDNA sample, 4 µL  $5 \times$  Green Go Taq Reaction Buffer 2 µL, 2.5 mM dNTPs Mix, 0.1 µL Go Taq polymerase (Promega, Madison, WI) and with specific primer sets (5 µM each). PCR products were electrophoresed in a 2% agarose gel and photographed under ultraviolet light. Each primer was designed to encompass an exon junction for prevention of templating possibly contaminated genomic DNA. These sense/antisense primers for PCR were designed as follows; (a) urokinase-type plasminogen activator (uPA), 5'-GCCATCCCGACTATACAGA-3'/ 5'-GTCAGCAGCACACAGCATT-3'; (b) urokinase-type plasminogen activator receptor (uPAR), 5'-TTA CCTCGAATGCATTTTCCT-3'/ 5'-TTGCACAGCC TCTTACCATA-3'; (c) Plasminogen activator inhibitor-1 (PAI-1), 5'-CAGCAGATTCAAGCAGCTAT G-3'/ 5'-TGTGTGTGTCTTCACCCAGTC-3'; (d) Heparanase (HPSE), 5'-ACTGGCAATCTCAAGTCAACCA-3'/ 5'-GCTCTCAACCACCTGGAAAAC T-3'; (e) Glyceraldehyde-3-phosphate dehydrogenase (G3PDH), 5'-TGAAGGTCGGAGTCAACGGAT TTGGT-3'/5'-CATGTGGGCCATGAGGTCCAC CAC-3'.

## RESULTS

**Establishment of DN mutant p53-expressing cell lines**  
To uncover the function of mutant *TP53* in tumor malignancy, we stably transfected NCI-H1299 cells which expressed no p53 protein, with mutant *TP53* expression vector, pIRES2-AcGFP1 p53 R248Q or pIRES2-AcGFP1 p53 R248W. For control, the cell line was transfected with pIRES2-AcGFP1 p53 (1-83) which encoded codon 1 to 83 of p53 protein. These vectors contain the internal ribosome entry sites (IRES) of the encephalomyocarditis virus between the multi-cloning site and the AcGFP1 (green fluorescence protein derived from *Aequorea coerulescens*) coding region, which permits both the gene of p53 and the AcGFP1 gene to be translated from a single bicistronic mRNA; therefore, the expression

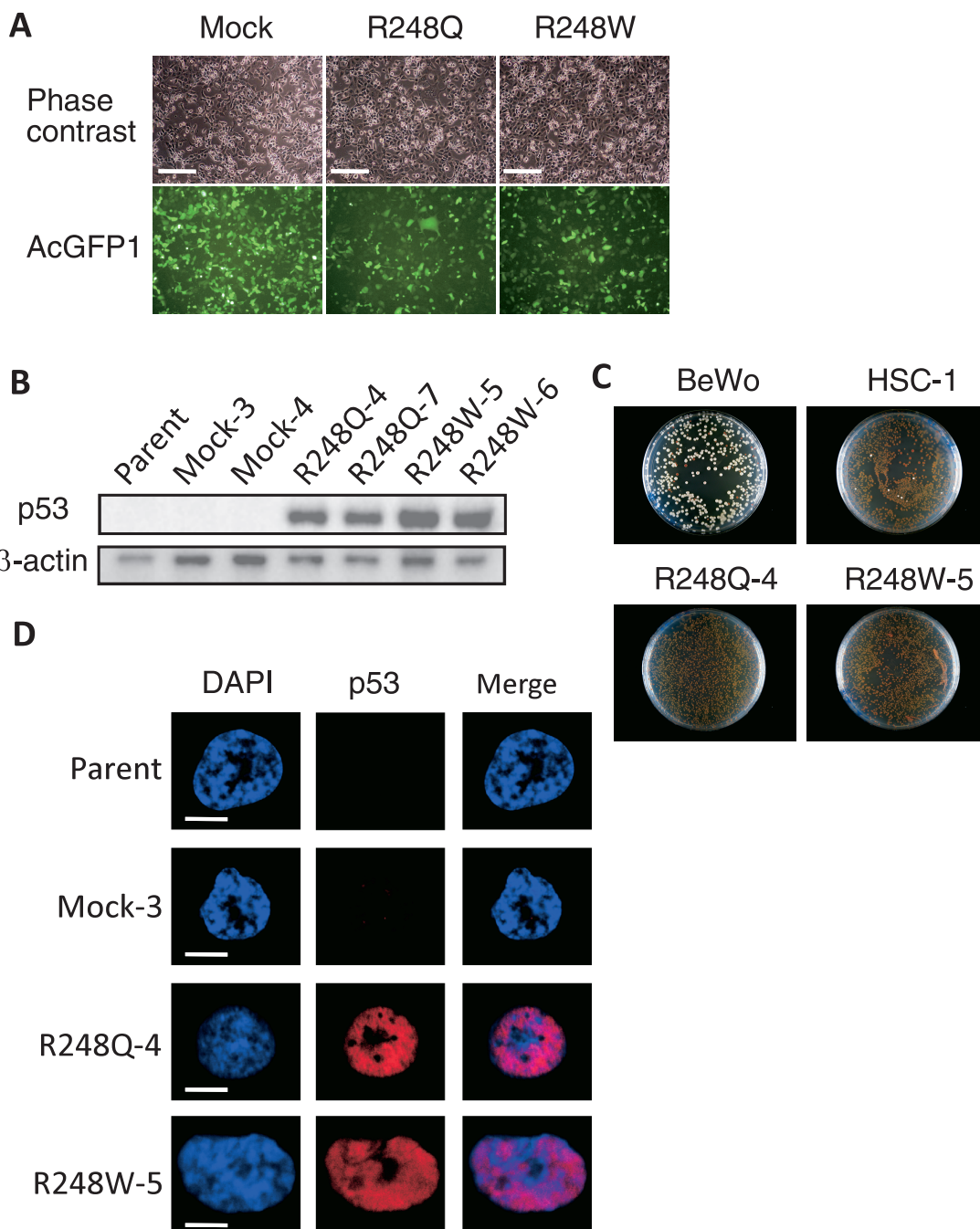


**Fig. 1** Expressions of mutant *TP53* in H1299 cells transfected with mutant *TP53* expression plasmid vectors. (A) Transfection efficiency of the mutant *TP53* expression vector (pTP53-R248Q or pTP53-R248W) or the control vector (pIRES2-AcGFP1-Δp53) into H1299 cells. The cells were observed under a phase contrast or a fluorescence inverted microscope 24 h after the transfection. The transfection efficiencies of pIRES2-AcGFP1-p53(1-83), pIRES2-AcGFP1 p53-R248Q and pIRES2-AcGFP1 p53-R248W were 87.5%, 94.2% and 90.4%, respectively. Scale bars represent 400 μm. (B) Western blot analysis of mutant *TP53* expression in the transfected cells. Proteins were extracted from the cells 24 h after the transfection with the expression vectors. (C) Yeast p53 functional assay of the cells transfected with pIRES2-AcGFP1 p53-R248Q or pIRES2-AcGFP1 p53-R248W, BeWo cells with wild type *TP53* and HSC-1 cells with mutant *TP53*. In this assay, yeast expressing mutant *TP53* forms red colonies whereas that expressing wild type *TP53* forms white colonies. (D) Laser confocal microscopic observation of mutant p53 proteins in the parental, Mock-transfectant, and mutant *TP53* transfectant NCI-H1299 cells. P53 proteins were visualized by indirect immunofluorescent staining using anti-p53 antibody and Alexa Fluor 568-conjugated anti-mouse IgG antibody. P53 proteins were localized in nuclei of the cells transfected with pIRES2-AcGFP1 p53-R248Q or pIRES2-AcGFP1 p53-R248W. Scale bars represent 10 μm.

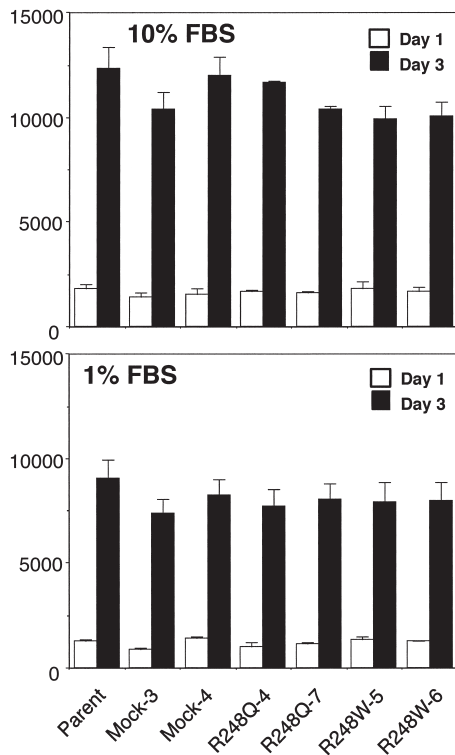


**Fig. 2** Mutant *TP53* does not affect the proliferation of NCI-H1299 cells. The cells ( $2 \times 10^3$ /well) were seeded on 96-well tissue culture plates. Cell proliferation assay was performed 1 and 3 days after the cell seeding. Data represent the mean  $\pm$  SD of triplicate samples.

of mutant *TP53* can be monitored by observing fluorescence of AcGFP1 under a fluorescence microscope. As shown in Fig. 1a, AcGFP1-positive were 87.5% of the cells transfected with pIRES2-AcGFP1 p53 (1-83) (Mock-transfectant), 94.2% of those transfected with pIRES2-AcGFP1 p53 R248Q (R248Q-transfectant), and 90.4% of those transfected with pIRES2-AcGFP1 p53 R248W (R248W-transfectant), indicating that these transfectants also expressed mutant *TP53* at similarly high rates. After the transfection, the cells were cultured in the presence of G418 sulfate for obtaining stably cloned transfectants: two cell lines cloned from Mock-transfectants were named Mock-3 and Mock-4; two cell lines from R248Q-transfectants, R248Q-4 and R248Q-7; two cell lines from R248W-transfectants, R248W-5 and R248W-6. We next examined by RT-PCR and Western blot analyses whether the transfectants expressed *TP53* gene. These analyses showed that the transfectants with pIRES2-AcGFP1 p53 R248Q or pIRES2-AcGFP1 p53 R248W, but neither parental nor the transfectants with pIRES2-AcGFP1 p53 (1-83), expressed p53 protein (Fig. 1B).

We further analyzed by yeast p53 functional assay to confirm that the former two transfectants produced mutant p53 proteins. The yeast p53 functional assay is a useful assay to evaluate the functional status of p53 protein by colony color (14). Namely, a yeast strain (yIG397) contains an integrated plasmid with a p53-responsive promoter-driving *ADE2* gene expression; this strain, containing wild-type p53, activates *ADE2* transcription and forms a white colony whereas a strain containing mutant p53 fails to activate *ADE2* transcription and forms a red colony. As shown in Fig. 1C, the yeast which was transformed with plasmid containing cDNA obtained from TP53 transcripts of the transfectants with pIRES2-AcGFP1 p53 R248Q or pIRES2-AcGFP1 p53 R248W formed red colonies. We further confirmed by sequence analysis that pSS16-based plasmids obtained from the yeast forming red colonies contained mutant *TP53* R248Q or R248W (data not shown).

#### *Intracellular localization of p53 in R248Q cells and R248W cells*

We next observed intracellular localization of p53 mutant proteins in R248Q- and R248W-transfected cells under a laser confocal microscope. Rightly, p53 was not detected in parental H1299 cells or Mock cells. In R248Q- and R248W-transfectants, the p53 proteins were observed in nuclei (Fig. 1D).

#### *Proliferative activity of NCI-H1299 cells expressing mutant p53*

We first investigated the proliferative activity of NCI-H1299 cells expressing mutant p53 by using a colorimetric crystal violet-staining method. The cells were cultured in the presence of 1% or 10% FBS. The assay was performed 1 and 3 days after the cell seeding. There was no significant difference in proliferative activity among the parent cells, the mock-transfectants, R248Q-transfectants and R248W-transfectants regardless of the difference of FBS concentration (Fig. 2).

#### *Invasive activity of NCI-H1299 cells expressing mutant p53*

To examine whether mutant p53 affected the invasive activity of H1299 cells, we carried out the *in vitro* invasion assay using Matrigel invasion chambers. Uncloned R248Q-transfectants showed significantly high invasive activity compared to the parent cells, mock-transfectants or R248W-transfectants in assay of a 24 h-incubation ( $P < 0.01$ , by Student's *t*-test) (Fig. 3A). Cloned R248Q-transfectants also

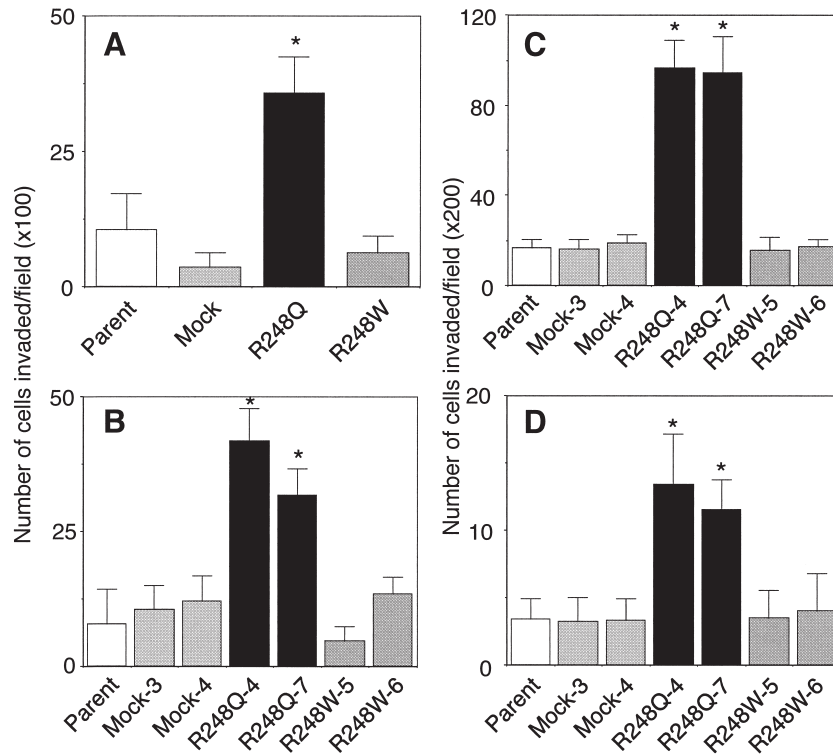


**Fig. 3** Invasiveness of parental H1299 cells and the transfectant cells. (A) Invasion of Matrigel by mutant *TP53*-transfected cells prior to cell cloning. (B) Invasion of Matrigel by cloned cells transfected with mutant *TP53*. (C) Invasion of type I collagen gel in the presence of 10% FBS by cloned cells transfected with mutant *TP53*. (D) Invasion of type I collagen gel in the absence of FBS by cloned cells transfected with mutant *TP53*. \*Statistically significant difference compared to the parental, Mock-transfected and pIRES2-AcGFP1 p53-R248W-transfected cells ( $P < 0.01$  by Student's *t*-test).

showed higher invasiveness than the parent cells or other transfectants ( $P < 0.01$ , by Student's *t*-test) (Fig. 3B). We next examined the invasion of type I collagen gel by the mutant *TP53*-transfectants. As shown in Fig. 3C and D, R248Q-transfectants had high potential to invade type I collagen gel compared to the parent cells or other transfectants regardless of the presence or absence of FBS in the assay system ( $P < 0.01$ , by Student's *t*-test).

#### *Migratory activity of NCI-H1299 cells expressing mutant p53*

Cell migratory activity and Matrigel degradation are essential for the cells to invade Matrigel. Therefore, we performed chemotaxis assay and *in vitro* wound healing assay to determine whether enhanced invasiveness of R248Q-transfectants was due to an increase in cell migratory activity. There was no significant difference in chemotactic activity between the R248Q-transfectants and other cells regardless of the chemoattractants (fibronectin, vitronectin, or laminin-1) (Fig. 4A, 4B and 4C). The result of *in vitro* wound healing assay showed that the migratory

activity of the two R248Q-transfectants was not always higher than that of any other cells (Fig. 5A and 5B).

#### *Expressions of extracellular matrix-degradative enzymes and their inhibitors in NCI-H1299 cells expressing mutant p53*

We next analyzed the expressions of extracellular matrix (ECM)-degradative enzymes and their inhibitors to determine whether enhanced invasiveness of R248Q-transfectants was due to alteration in those. The expression levels of 14 matrix metalloproteinases (MMPs), 4 tissue inhibitors of MMP (TIMP), and reversion-inducing cysteine-rich protein with Kazal motifs (RECK) were quantified by a real-time RT-PCR method. As shown in Fig. 6A, there was no particular gene of which expression was altered by p53 R248Q expression in NCI-H1299 cells. The expression levels of ECM-degradative enzymes and their inhibitors such as *uPA*, *uPAR*, *PAI-1* and *HPSE* in R248Q-transfectants did not differ from those in parent cells or other transfectants (Fig. 6B).

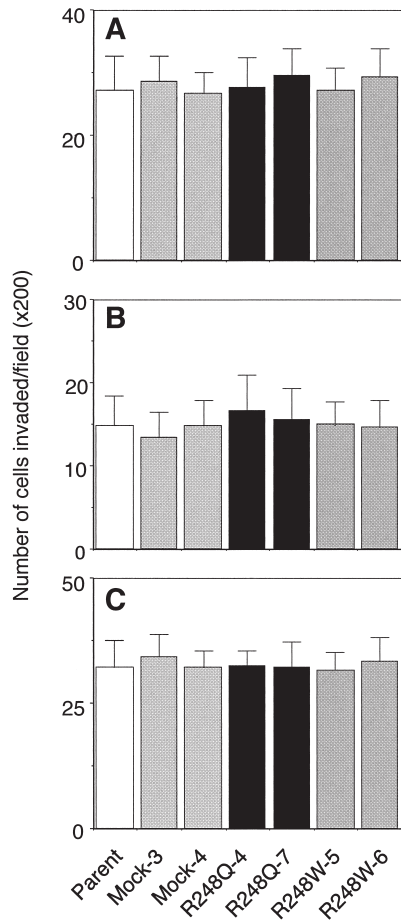


**Fig. 4** Migratory activities of parental and the transfectant cells toward fibronectin, vitronectin or laminin-1 in a chemotaxis assay. Chemotaxis assay was performed for 6 h by using Transwell chambers. Chemotactic activity of the parental, mutant *TP53*-transfected, and Mock-transfected cells toward fibronectin (A), vitronectin (B) and laminin-1 (C).

## DISCUSSION

Mutations most frequently occur in the *TP53* gene, encoding the p53 tumor suppressor, in human cancers. It is well known that p53 mutations result not only in loss of anti-oncogenic activities but also in trans-dominant inactivation of the remaining wild-type p53 (19). In addition, several p53 mutants acquire novel oncogenic functions (GOF) (3). In the present study, we examined the contribution of p53 mutations occurred at codon 248 to *in vitro* malignant properties of tumor cells through the GOF properties. And we found that R248Q but not R248W mutation conferred more invasive potential on p53-null H1299 cells. It is for the first time to reveal that the distinct mutations, even if the mutations occurred at the same codon, gave tumor cells

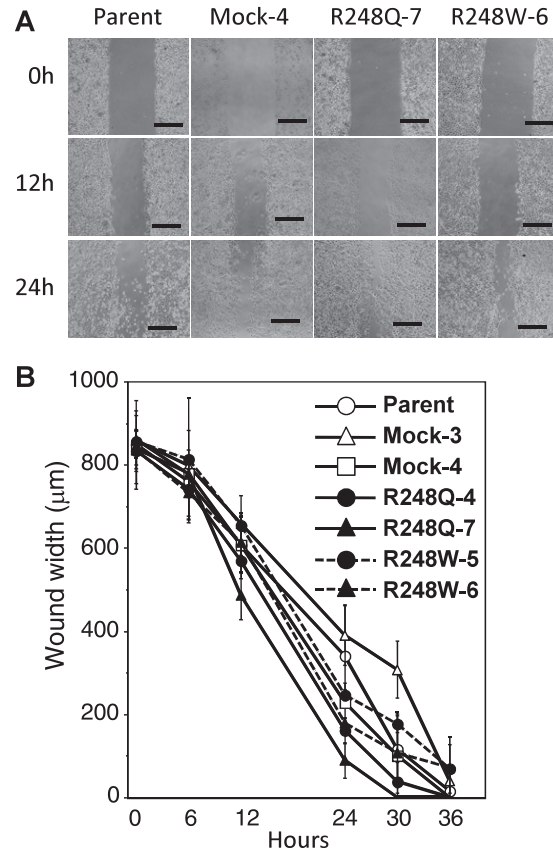


**Fig. 5** Migratory activities of parental H1299 cells and transfectant cells in an *in vitro* wound-healing assay. (A) Microphotographs of monolayer cultures of cloned R248Q-transfected (R248Q-7), R248W-transfected (R248W-6) and Mock-transfected (Mock-4), and parental cells at 0, 12 and 24 h after the scratching the monolayers with a pipet tip. Scale bars represent 500 μm. (B) Chronological changes of distances between two “wound” edges. Data represent the mean ± SD of 10 sites where the distances were measured with a micrometer.

different *in vitro* malignant properties.

We have previously reported that both R248Q and R248W p53 mutants lacked sequence-specific DNA binding and inhibited transactivation of p73beta which is one of p53 family members (10, 15). There are some reports indicating that R248W mutant reduced the transcriptional activity of p73alpha (4) or p63 (23) although R248Q mutant was not examined there. Thus there is no evidence, so far, to elucidate the functional difference between R248Q and R248W p53 mutants in H1299 transfectants. Noskov *et al.* showed a difference of protein structure between R248Q and R248W mutants by using molecular dynamics simulations (16). They indicated that R248Q did not bind to the DNA sequences recognized by wild type p53 mainly due to the loss of

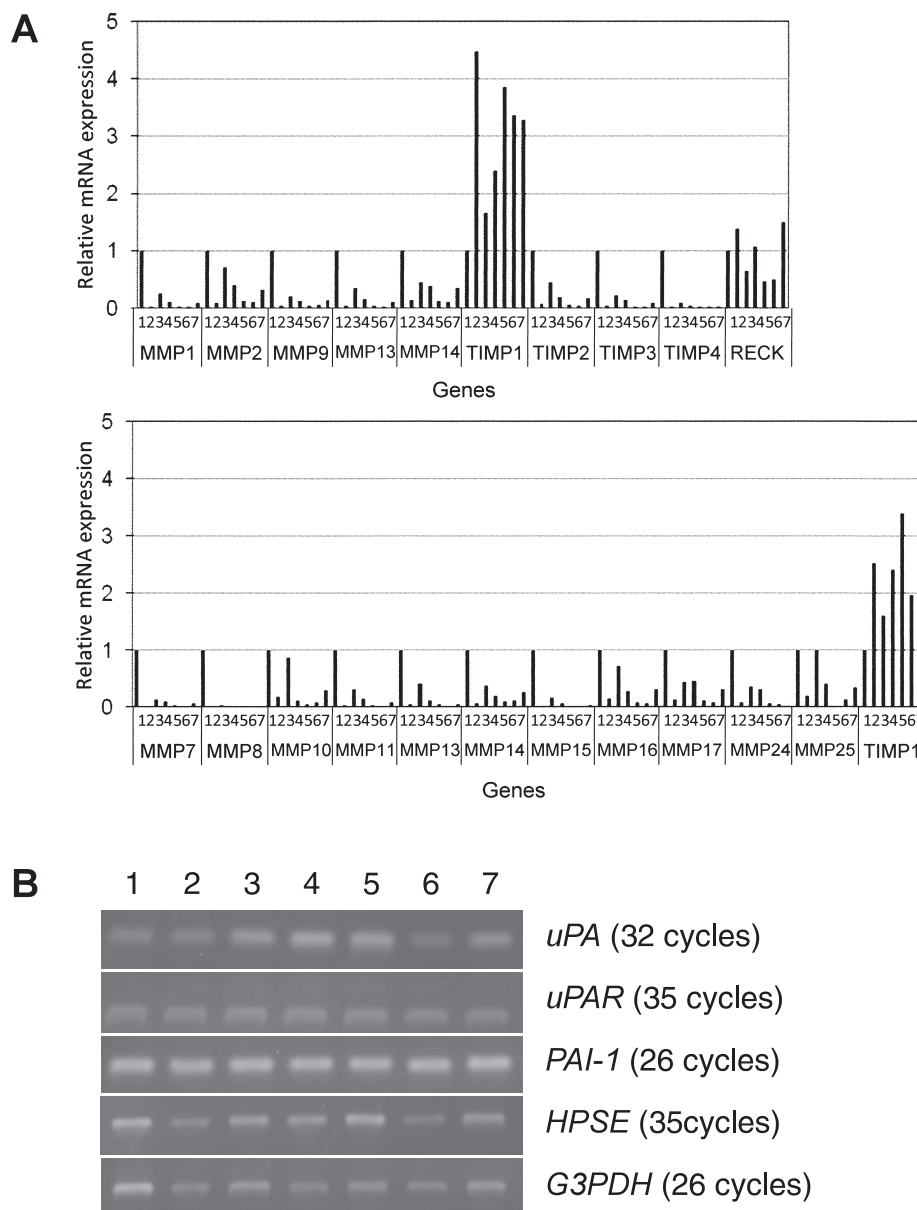


**Fig. 6** Expressions of matrix metalloproteinases (MMPs) and their inhibitors in parental H1299 cells and the transfectant cells. (A) The relative levels of mRNA of MMPs and their inhibitors were determined by a real-time RT-PCR method. (B) Expression levels of mRNA of urokinase-type plasminogen activator (*uPA*), uPA receptors (*uPAR*), plasminogen activator inhibitor-1 (*PAI-1*), heparanase (*HPSE*), and glyceraldehyde-3-phosphate dehydrogenase (*G3PDH*) in parental H1299 cells and the transfectant cells. The expression levels were analyzed by a RT-PCR method. The PCR products were electrophoresed and stained with ethidium bromide. 1: parent, 2: Mock-3, 3: Mock-4, 4: R248Q-4, 5: R248Q-7, 6: R248W-5, 7: R248W-6.

major groove contacts from K120, besides due to unfavorable interactions of D281, whereas R248W did not mainly due to the loss of minor groove contacts from the mutant residue itself. Recently Merabet *et al.* also reported the structural and biochemical difference between R248Q and R248W (11). Such a difference of structural changes by substitution of one amino acid indicates the possibility

that each mutant regulates the transcription of different kinds of genes, which results in the different invasiveness.

We speculated that the R248Q mutant acquired a new function as a transcription factor which regulated the expressions of invasion-related genes, since the mutant protein was observed only in the nuclei of H1299 transfectants. Therefore, we compared

changes of phenotypes and expressions of genes related to invasion between R248Q- and R248W-transfectants; we analyzed especially cell motility and the expressions of genes involved in degradation of ECM. There was no difference between R248Q- and R248W-transfectants in cell motility which was measured by chemotaxis and wound healing assays. It suggests that enhancement of invasiveness by the expression of R248Q was not due to an increase in cell motile activity. We next examined the involvement of an increased ability to digest the components of ECM in the invasiveness enhanced by R248Q. Unfortunately, however, we could not find R248Q-specific changes in the expressions of the genes related to ECM-degradation such as MMPs, uPA and heparanase, and their inhibitors such as TIMPs, RECK and PAI-1. From these findings, we cannot so far identify any specific invasion-related molecules of which expressions or functions are regulated by R248Q but not R248W. It is further necessary to monitor effects of R248Q-transduction on a global gene expression by using a cDNA microarray or a tiling array combined with chromatin-immunoprecipitation in order to discover the molecules involved in R248Q-dependent invasion. Overall, the findings here indicate that the activity of GOF of p53 mutants is different even if the mutations occur at the same codon and that the status of p53 including the GOF activity as well as transdominancy should be considered in diagnosis and therapy.

#### Acknowledgement

The authors thank Ms. Yanome for her help in preparing the manuscript. The authors have no financial relationships to disclose.

#### REFERENCES

- Asano T, Tada M, Cheng S, Takemoto N, Kuramae T, Abe M, Takahashi O, Miyamoto M, Hamada J, Moriuchi T and Kondo S (2008) Prognostic values of matrix metalloproteinase family expression in human colorectal carcinoma. *J Surg Res* **146**, 32–42.
- Brachmann RK, Vidal M and Boeke JD (1996) Dominant-negative p53 mutations selected in yeast hit cancer hot spots. *Proc Natl Acad Sci USA* **93**, 4091–4095.
- Brosh R and Rotter V (2009) When mutants gain new powers: news from the mutant p53 field. *Nat Rev Cancer* **9**, 701–713.
- Di Como CJ, Gaidon C and Prives C (1999) p73 function is inhibited by tumor-derived p53 mutants in mammalian cells. *Mol Cell Biol* **19**, 1438–1449.
- Flaman JM, Frebourg T, Moreau V, Charbonnier F, Martin C, Chappuis P, Sappino AP, Limacher IM, Bron L, Benhattar J, Tada M, VanMeir EG, Estreicheru A and Iggo RD (1995) A simple p53 functional assay for screening cell lines, blood, and tumors. *Proc Natl Acad Sci USA* **92**: 3963–3967.
- Frazier MW, He X, Wang J, Gu Z, Cleveland JL and Zambetti GP (1998) Activation of c-myc gene expression by tumor-derived p53 mutants requires a discrete C-terminal domain. *Mol Cell Biol* **18**, 3735–3743.
- Hainaut P and Hollstein M (2000) p53 and human cancer: the first ten thousand mutations. *Adv Cancer Res* **77**, 81–137.
- Hassan NM, Tada M, Hamada J, Kashiwazaki H, Kameyama T, Akhter R, Yamazaki Y, Yano M, Inoue N and Moriuchi T (2008) Presence of dominant negative mutation of TP53 is a risk of early recurrence in oral cancer. *Cancer Lett* **270**, 108–119.
- Kueng W, Silber E and Eppenberger U (1989) Quantification of cells cultured on 96-well plates. *Anal Biochem* **182**, 16–19.
- Marutani M, Tonoki H, Tada M, Takahashi M, Kashiwazaki H, Hida Y, Hamada J, Asaka M and Moriuchi T (1999) Dominant-negative mutations of the tumor suppressor p53 relating to early onset of glioblastoma multiforme. *Cancer Res* **59**, 4765–4769.
- Merabet A, Houleberghs H, Maclagan K, Akanho E, Bui TT, Pagano B, Drake AF, Fraternali F and Nikolova PV (2010) Mutants of the tumour suppressor p53 L1 loop as second-site suppressors for restoring DNA binding to oncogenic p53 mutations: structural and biochemical insights. *Biochem J* **427**, 225–236.
- Milner J and Medcalf EA (1991) Cotranslation of activated mutant p53 with wild type drives the wild-type p53 protein into the mutant conformation. *Cell* **65**, 765–774.
- Milner J, Medcalf EA and Cook AC (1991) Tumor suppressor p53: analysis of wild-type and mutant p53 complexes. *Mol Cell Biol* **11**, 12–19.
- Miyazaki YJ, Hamada J, Tada M, Furuuchi K, Takahashi Y, Kondo S, Katoh H and Moriuchi T (2002) HOXD3 enhances motility and invasiveness through the TGF-beta-dependent and -independent pathways in A549 cells. *Oncogene* **21**, 798–808.
- Monti P, Campomenosi P, Ciribilli Y, Iannone R, Aprile A, Inga A, Tada M, Menichini P, Abbondandolo A and Fronza G (2003) Characterization of the p53 mutants ability to inhibit p73 beta transactivation using a yeast-based functional assay. *Oncogene* **22**, 5252–5260.
- Noskov SY, Wright JD and Lim C (2002) Long-range effects of mutating R248 to Q/W in the p53 core domain. *J Phys Chem* **106**, 13047–13057.
- Ohta H, Hamada J, Tada M, Aoyama T, Furuuchi K, Takahashi Y, Totsuka Y and Moriuchi T (2006) HOXD3-overexpression increases integrin alpha v beta 3 expression and deprives E-cadherin while it enhances cell motility in A549 cells. *Clin Exp Metastasis* **23**, 381–390.
- Oren M (2003) Decision making by p53: life, death and cancer. *Cell Death Differ* **10**, 431–442.
- Petitjean A, Achatz MI, Borresen-Dale AL, Hainaut P and Olivier M (2007) TP53 mutations in human cancers: functional selection and impact on cancer prognosis and outcomes. *Oncogene* **26**, 2157–2165.
- Petitjean A, Mathe E, Kato S, Ishioka C, Tavtigian SV, Hainaut P and Olivier M (2007) Impact of mutant p53 functional properties on TP53 mutation patterns and tumor phenotype: lessons from recent developments in the IARC TP53 database. *Hum Mutat* **28**, 622–629.
- Sakuragi N, Watari H, Ebina Y, Yamamoto R, Steiner E,

- Koelbl H, Yano M, Tada M and Moriuchi T (2005) Functional analysis of p53 gene and the prognostic impact of dominant-negative p53 mutation in endometrial cancer. *Int J Cancer* **116**, 514–519.
22. Sampath J, Sun D, Kidd VJ, Grenet J, Gandhi A, Shapiro LH, Wang Q, Zambetti GP and Schuetz JD (2001) Mutant p53 cooperates with ETS and selectively up-regulates human MDR1 not MRP1. *J Biol Chem* **276**, 39359–39367.
23. Strano S, Fontemaggi G, Costanzo A, Rizzo MG, Monti O, Baccarini A, Del Sal G, Levrero M, Sacchi A, Oren M and Blandino G (2002) Physical interaction with human tumor-derived p53 mutants inhibits p53 activities. *J Biol Chem* **277**, 18817–18826.
24. Tada M, Iggo RD, Ishii N, Shinohe Y, Sakuma S, Estreicher A, Sawamura Y and Abe H (1996) Clonality and stability of the p53 gene in human astrocytic tumor cells: quantitative analysis of p53 gene mutations by yeast functional assay. *Int J Cancer* **67**, 447–450.
25. Weisz L, Zalcenstein A, Stambolsky P, Cohen Y, Goldfinger N, Oren M and Rotter V (2004) Transactivation of the EGR1 gene contributes to mutant p53 gain of function. *Cancer Res* **64**, 8318–8327.
26. Zalcenstein A, Stambolsky P, Weisz L, Müller M, Wallach D, Goncharov TM, Krammer PH, Rotter V and Oren M (2003) Mutant p53 gain of function: repression of CD95(Fas/APO-1) gene expression by tumor-associated p53 mutants. *Oncogene* **22**, 5667–5676.